

# Simultaneous Assessment of Myocardial Free Fatty Acid Utilization and Left Ventricular Function Using $^{123}\text{I}$ -BMIPP-Gated SPECT

Masayuki Inubushi, Eiji Tadamura, Takashi Kudoh, Naoya Hattori, Shigeto Kubo, Takaaki Koshiji, Kazunobu Nishimura, Masashi Komeda, Nagara Tamaki and Junji Konishi

Department of Nuclear Medicine and Diagnostic Imaging, and Department of Cardiovascular Surgery, Kyoto University Faculty of Medicine, Kyoto; Department of Nuclear Medicine, Hokkaido University, Sapporo, Japan

This study was designed to evaluate the methodological feasibility of  $^{123}\text{I}$ -labeled  $\beta$ -methyl-p-iodophenyl-pentadecanoic acid (BMIPP)-gated SPECT to assess regional and global left ventricular (LV) function in comparison with  $^{99\text{m}}\text{Tc}$ -sestamibi (methoxyisobutyl isonitrile [MIBI])-gated SPECT and first-pass radionuclide angiography (FPRNA). **Methods:** Forty-four patients with stable coronary artery disease underwent rest BMIPP-gated SPECT (111 MBq, 60 s/step) and rest MIBI-gated SPECT (600 MBq, 40 s/step) within a week. From both gated SPECT studies, regional defect scores (DS), wall motion scores (WMS) and wall-thickening scores (WTS) were evaluated visually using 4-point scales for nine segments, and LV ejection fraction (EF) (%) was automatically calculated using Quantitative Gated SPECT (QGS) software. FPRNA was also performed on injection of MIBI. **Results:** Exact agreement between the two gated SPECT studies was 84.1% ( $\kappa = 0.706$ ,  $r = 0.907$ ,  $P < 0.0001$ ) in WMS and 87.1% ( $\kappa = 0.662$ ,  $r = 0.884$ ,  $P < 0.0001$ ) in WTS. LVEF obtained from BMIPP-gated SPECT linearly correlated with those from MIBI-gated SPECT ( $y = -0.27 + 0.944x$ ,  $r = 0.948$ ,  $\text{SEE} = 5.00$ ,  $P < 0.0001$ ) and FPRNA ( $y = -7.32 + 1.042x$ ,  $r = 0.919$ ,  $\text{SEE} = 6.19$ ,  $P < 0.0001$ ). Even in 21 patients with mismatch segments (BMIPP DS > MIBI DS), agreement was considered to be acceptable in WMS (81.5%,  $\kappa = 0.707$ ,  $r = 0.853$ ,  $P < 0.0001$ ) and in WTS (76.7%,  $\kappa = 0.526$ ,  $r = 0.754$ ,  $P < 0.0001$ ), and correlation in LVEF remained good between BMIPP-gated SPECT and MIBI-gated SPECT ( $y = -1.24 + 0.955x$ ,  $r = 0.938$ ,  $\text{SEE} = 6.25$ ,  $P < 0.0001$ ) or FPRNA ( $y = -6.03 + 1.024x$ ,  $r = 0.913$ ,  $\text{SEE} = 7.38$ ,  $P < 0.0001$ ). **Conclusion:** BMIPP-gated SPECT can evaluate regional and global LV function with the QGS software. Therefore, BMIPP-gated SPECT offers the opportunity for simultaneous assessment of myocardial free fatty acid utilization and LV function.

**Key Words:** gated SPECT;  $^{123}\text{I}$ - $\beta$ -methyl-p-iodophenyl-pentadecanoic acid;  $^{99\text{m}}\text{Tc}$ -sestamibi; first-pass radionuclide angiography; left ventricular function

J Nucl Med 1999; 40:1840-1847

**G**ated SPECT using  $^{99\text{m}}\text{Tc}$ -labeled myocardial perfusion tracers, such as  $^{99\text{m}}\text{Tc}$ -sestamibi (methoxyisobutyl isonitrile [MIBI]), has been shown to provide useful information about myocardial perfusion and left ventricular (LV) function on one imaging sequence (1-3). Although the clinical value of  $^{123}\text{I}$ - $\beta$ -methyl-iodophenyl-pentadecanoic acid (BMIPP) has been widely recognized (4-21), BMIPP-gated SPECT has never been reported, because  $^{123}\text{I}$ -labeled tracers are not as ideal for gated SPECT imaging as  $^{99\text{m}}\text{Tc}$ -based agents, mainly due to the limited photon density in the myocardium. Germano et al. (22), Cedars-Sinai Medical Center group, developed a superior edge detection algorithm and perfectly automatic Quantitative Gated SPECT (QGS) software to measure LV ejection fraction (EF) from MIBI-gated SPECT images. This algorithm has been successfully applied to relatively lower-count images by fast acquisition MIBI-gated SPECT (23) or  $^{201}\text{Tl}$ -gated SPECT (24). This study was designed to evaluate the methodological feasibility of BMIPP-gated SPECT to assess regional and global LV function in comparison with MIBI-gated SPECT and first-pass radionuclide angiography (FPRNA).

## MATERIALS AND METHODS

### Patients

Forty-four consecutive patients with stable coronary artery disease (CAD) were studied between August 1997 and June 1998. The patient profile is summarized in Table 1.

### Study Protocol

All patients underwent rest BMIPP- and rest MIBI-gated SPECT within a week of one another. FPRNA was also performed on injection of MIBI.

### Rest Gated SPECT Using BMIPP and MIBI

All SPECT data were acquired on a rotating dual-head gamma camera (VariCam; Elscint Ltd., Haifa, Israel) equipped with low-energy, high-resolution (LEHR) collimators.

After they fasted overnight, patients at rest were injected with 111 MBq BMIPP. Gated SPECT was performed 15 min later. A total of 30 projections were obtained over  $180^\circ$  from the right anterior oblique view to the left posterior oblique view in the

Received Sep. 16, 1998; revision accepted Mar. 30 1999.

For correspondence or reprints contact: Masayuki Inubushi, MD, Department of Nuclear Medicine and Diagnostic Imaging, Kyoto University Faculty of Medicine, 54 Shogoin-Kawahara Sakyo, Kyoto 606-8507, Japan.

**TABLE 1**  
Patient Characteristics

Characteristic	No.
Number of patients	44
Men	37
Women	7
Age (y)	66 ± 8
Height (cm)	160 ± 6
Weight (kg)	58 ± 11
Clinical diagnosis	
Angina pectoris (AP)	23
Old myocardial infarction (OMI)	12
OMI with AP	9
Number of diseased coronary arteries	
One vessel	4
Two vessels	15
Three vessels	25
Mean	2.5 ± 0.7
History of coronary revascularization	
Yes	27
No	17

159-keV photopeak with a  $\pm 10\%$  window and a 60-s acquisition time per projection, distributed over eight cardiac frames. The acceptance window of cardiac beat length was set to its maximum value of 100%. The total acquisition time was about 16 min including rotating time.

MIBI-gated SPECT was also acquired in all patients within a week (3–7 d) after BMIPP-gated SPECT. Gated SPECT was performed 1 h after injection of 600 MBq MIBI at rest. The acquisition condition was the same as that of BMIPP-gated SPECT, except there was a 140-keV photopeak with a  $\pm 10\%$  window and a 40-s acquisition time per projection. The total acquisition time was about 11 min.

The projection datasets were prefiltered with a two-dimensional Butterworth filter (order 5, critical frequency 0.40 [BMIPP] or 0.45 [MIBI] cycles/pixel, pixel size 7.2 mm) and were reconstructed with filtered backprojection (ramp filter) and without attenuation correction.

#### Data Analysis of Gated SPECT

The LV myocardium was divided into nine segments (Fig. 1). Regional defect scores of BMIPP and MIBI were visually assessed using a 4-point scale for each segment on nongated images

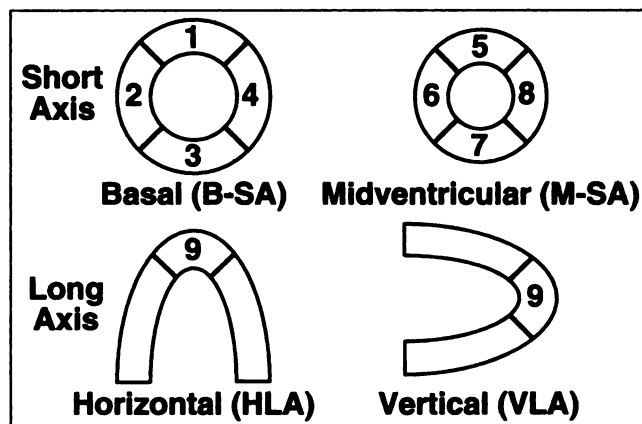


**FIGURE 1.** Segmentation scheme used for regional assessment of defect scores, wall motion and wall thickening on SPECT.

summed from all cardiac cycle images (0 = normal, 1 = mildly reduced, 2 = moderately reduced and 3 = absent). Endocardial and epicardial surfaces were estimated and were displayed for all gating intervals in the cardiac cycle using Germano's QGS software without any operator interaction in the same condition for both gated SPECT images. Regional wall motion was scored visually on a 4-point scale using a smoothed cinematic display (0 = normal, 1 = mild hypokinesis, 2 = moderate to severe hypokinesis and 3 = akinesis or dyskinesis). Regional wall thickening was also scored visually on a 4-point scale based on myocardial wall brightening from diastole to systole (0 = normal, 1 = mildly impaired, 2 = moderately impaired and 3 = severely impaired to absent thickening). Visual assessments were all determined by consensus of two expert observers without knowledge of clinical information. LVEF was automatically calculated from the relative end-diastolic and end-systolic volume.

#### First-Pass Radionuclide Angiography

On injection of 600 MBq MIBI for SPECT imaging, FPRNA data were also acquired to measure LVEF in the anterior view with a multicrystal gamma camera (SIM-400; Scintacor, Milwaukee, WI) equipped with a high-sensitivity parallel-hole collimator (25,26). The matrix size was  $20 \times 20$  pixels, with center-to-center pixel spacing of 10 mm. The time intervals were 25 ms. The acquired data were stored in a Macintosh computer and were processed for LVEF with commercially available software as previously described (27,28).

#### Mismatch Between BMIPP and MIBI SPECT

A segment with a greater defect score on BMIPP SPECT than on MIBI SPECT was defined as mismatch. The patients were divided into two groups: patients with at least one mismatch segment (mismatch) and those without (match).

#### Statistical Analysis

Data are expressed as mean  $\pm 1$  SD. Proportions and continuous variables were analyzed with Student *t* test, Wilcoxon signed rank test or Mann-Whitney test. The agreement among regional functional measurements and myocardial uptake scores obtained from BMIPP- and MIBI-gated SPECT was evaluated from  $4 \times 4$  contingency tables using  $\kappa$  statistics (29), Spearman's rank coefficient and chi-square analyses. In general, a  $\kappa$  value of 0.6 or greater is considered indicative of good agreement. The agreement of LVEF values derived from gated SPECT and FPRNA was assessed using linear regression and Bland-Altman analyses (30,31). A *P* value less than 0.05 was considered to be significant.

#### RESULTS

No patient showed clinical signs or evidence of anginal attacks during the period of the study protocol.

The total myocardial counts on BMIPP and MIBI nongated SPECT images were  $562 \pm 114$  kcts and  $1122 \pm 266$  kcts, respectively ( $P < 0.0001$ ). Despite lower total BMIPP myocardial counts, the quality of BMIPP-gated SPECT images was recognized to be adequate for interpretation in all patients by the two expert observers, and endocardial and epicardial contours were generated automatically, even in the apparent absence of tracer uptake (Fig. 2).

FPRNA also showed good quality for clear identification of the end-diastolic and end-systolic phases in all patients.

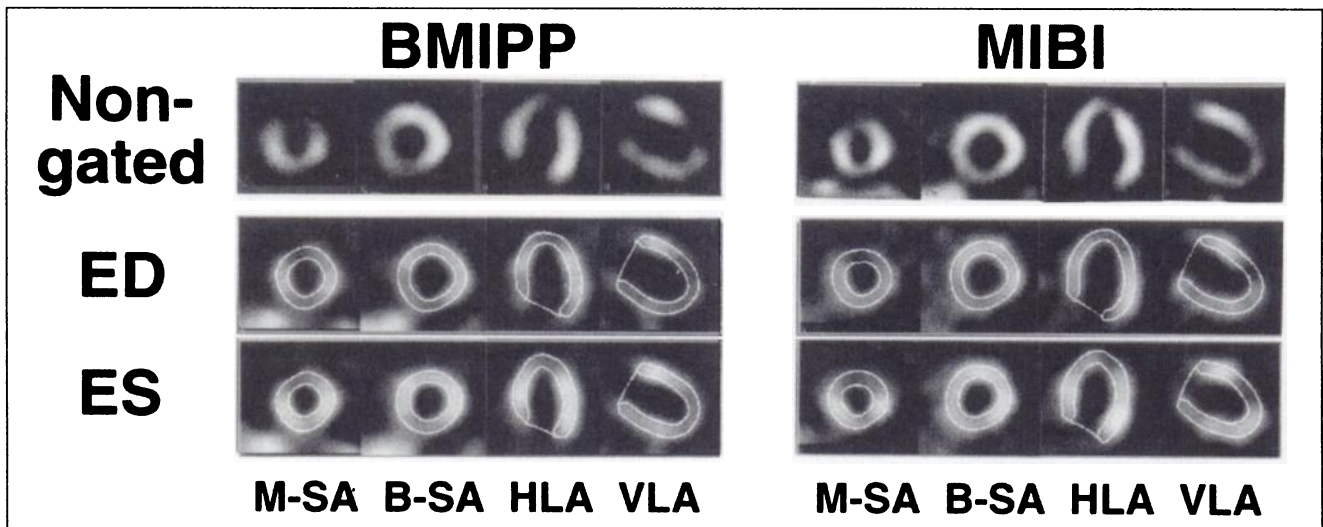


**FIGURE 2.** Summed nongated, end-diastolic (ED) and end-systolic (ES) images from  $^{123}\text{I}$ -BMIPP- and  $^{99\text{m}}\text{Tc}$ -methoxyisobutyl isonitrile (MIBI)-gated SPECT of representative case with large scar in anterior wall and mismatch area in septal wall.

No patient had to be excluded because of severe arrhythmia or poor patient positioning during FPRNA acquisition.

#### Mismatch Between BMIPP and MIBI SPECT

Mismatch was found in 40 (10.1%) of 396 segments and in 21 (47.7%) of 44 patients. The patient profile is shown in Table 2.

#### Correlation in Wall Motion and Wall-Thickening Scores

In 396 segments of all 44 patients, exact agreement between BMIPP- and MIBI-gated SPECT studies was 84.1% in wall motion scores ( $\kappa = 0.706$ ,  $r = 0.907$ ,  $P < 0.0001$ ) and 87.1% in wall-thickening scores ( $\kappa = 0.662$ ,  $r = 0.884$ ,  $P < 0.0001$ ), and agreement within one rank was 98.7% and 98.0%, respectively (Table 3). In 189 segments of mismatch patients, exact agreement was 81.5% in wall motion scores ( $\kappa = 0.707$ ,  $r = 0.853$ ,  $P < 0.0001$ ) and 76.7% in wall-thickening scores ( $\kappa = 0.526$ ,  $r = 0.754$ ,  $P < 0.0001$ ), and agreement within one rank was 97.9% and 95.8%, respectively (Table 4). In 207 segments of match patients, exact agreement was 86.4% in wall motion scores ( $\kappa = 0.684$ ,  $r = 0.923$ ,  $P < 0.0001$ ) and 96.6% in wall-thickening scores ( $\kappa = 0.870$ ,  $r = 0.962$ ,  $P < 0.0001$ ), and agreement within one rank was 99.5% and 100%, respectively (Table 5).

#### Correlation in Left Ventricular Ejection Fraction

In overall analysis of 44 patients, LVEF obtained from BMIPP-gated SPECT linearly correlated well with LVEF from MIBI-gated SPECT ( $y = -0.27 + 0.944x$ ,  $r = 0.948$ ,  $\text{SEE} = 5.00$ ,  $P < 0.0001$ ) and FPRNA ( $y = -7.32 + 1.042x$ ,  $r = 0.919$ ,  $\text{SEE} = 6.19$ ,  $P < 0.0001$ ). In 21 mismatch patients, correlation in LVEF remained good between BMIPP-gated SPECT and MIBI-gated SPECT ( $y = -1.24 + 0.955x$ ,  $r = 0.938$ ,  $\text{SEE} = 6.25$ ,  $P < 0.0001$ ) or FPRNA ( $y = -6.03 + 1.024x$ ,  $r = 0.913$ ,  $\text{SEE} = 7.38$ ,  $P < 0.0001$ ), as well as in 23 match patients. Bland-Altman analysis revealed no significant degree of systematic measurement bias in any patient group (Figs. 3 and 4).

#### Relationship Between Regional Myocardial Uptake and Left Ventricular Function

Regional defect scores significantly correlated with regional wall motion and thickening scores on both BMIPP- and MIBI-gated SPECT (Tables 6 and 7). The correlation

**TABLE 2**  
Patient Characteristics of Mismatch and Match Patients

Characteristic	Mismatch patients	Match patients	<i>P</i>
Number of patients	21	23	
Male	16	21	
Female	5	2	ns
Age (y)	65 ± 8	68 ± 8	ns
Height (cm)	160 ± 7	160 ± 5	ns
Weight (kg)	57 ± 13	58 ± 9	ns
Clinical diagnosis			ns
Angina pectoris (AP)	10	13	
Old myocardial infarction (OMI)	7	5	
OMI with AP	4	5	
Number of diseased coronary arteries			ns
One vessel	0	4	
Two vessels	8	7	
Three vessels	13	12	
Mean	2.6 ± 0.5	2.4 ± 0.8	
History of coronary revascularization			
Yes	17	10	
No	4	13	0.011
Total defect score of MIBI	3.4 ± 2.9	2.7 ± 3.0	ns
Total defect score of BMIPP	5.5 ± 3.1*	2.7 ± 3.0	0.038
Number of mismatch segments	1.9 ± 1.0	0	<0.0001

\*Versus total defect score of MIBI,  $P < 0.0001$ .

ns = not significant; MIBI = methoxyisobutyl isonitrile; BMIPP =  $\beta$ -methyl-p-iodophenyl-pentadecanoic acid.

**TABLE 3**

Relationship in Regional Functional Scores Between BMIPP- and MIBI-Gated SPECT in All Patients

BMIPP functional scores	MIBI functional scores				Total
	0	1	2	3	
0	237/289	5/7	2/0	0/0	244/296
1	23/20	55/36	4/1	0/0	82/57
2	1/4	12/8	24/12	3/1	40/25
3	0/3	2/1	11/6	17/8	30/18
Total	261/316	74/52	41/19	20/9	396/396

BMIPP =  $\beta$ -methyl-p-iodophenyl-pentadecanoic acid; MIBI = methoxyisobutyl isonitrile.

Numbers of segments were expressed as wall motion score/wall-thickening score. Wall motion scores,  $\kappa = 0.706$ ,  $r = 0.907$ ,  $P < 0.0001$ ; wall-thickening scores,  $\kappa = 0.662$ ,  $r = 0.884$ ,  $P < 0.0001$ .

**TABLE 5**

Relationship in Regional Functional Scores Between BMIPP- and MIBI-Gated SPECT in Match Patients

BMIPP functional scores	MIBI functional scores				Total
	0	1	2	3	
0	146/174	2/0	0/0	0/0	148/174
1	12/6	18/15	1/0	0/0	31/21
2	0/0	5/1	9/6	2/0	16/7
3	0/0	1/0	5/0	6/5	12/5
Total	158/180	26/16	15/6	8/5	207/207

BMIPP =  $\beta$ -methyl-p-iodophenyl-pentadecanoic acid; MIBI = methoxyisobutyl isonitrile.

Numbers of segments were expressed as wall motion score/wall-thickening score. Wall motion scores,  $\kappa = 0.684$ ,  $r = 0.923$ ,  $P < 0.0001$ ; wall-thickening scores,  $\kappa = 0.870$ ,  $r = 0.962$ ,  $P < 0.0001$ .

coefficients were higher in both analyses of wall motion and thickening scores on BMIPP-gated SPECT (wall motion scores,  $\kappa = 0.211$ ,  $r = 0.325$ ; wall-thickening scores,  $\kappa = 0.275$ ,  $r = 0.495$ ) than on MIBI-gated SPECT (wall motion scores,  $\kappa = 0.171$ ,  $r = 0.274$ ; wall-thickening scores,  $\kappa = 0.261$ ,  $r = 0.390$ ).

**DISCUSSION**

To date, gated SPECT technique has been widely used in clinical routine SPECT studies. However, gated SPECT has been exclusively performed using perfusion tracers. To our knowledge, this is the first validation of the accuracy of functional assessment when applying the gated technique to a unique metabolic tracer, BMIPP.

The present data demonstrated that there was a high degree of correlation in wall motion and thickening scores between BMIPP- and MIBI-gated SPECT. EF values obtained from BMIPP-gated SPECT correlated well with those from well-established methods of MIBI-gated SPECT and FPRNA. These results indicate that the regional and global

LV function can be accurately assessed with BMIPP-gated SPECT when processed with Germano's algorithm.

**Functional Assessment Using BMIPP-Gated SPECT**

EF values obtained from BMIPP-gated SPECT correlated well with those from MIBI-gated SPECT and FPRNA in match and mismatch patients. This fact confirms the value of QGS software when applied to low count images with areas of reduced tracer uptake.

On the other hand, our data showed that the correlation of wall-thickening scores between the two gated SPECT studies in mismatch patients was not as good as that in match patients. The wall-thickening assessment on BMIPP-gated SPECT may be intrinsically limited in mismatch segments, because wall thickening was evaluated with a visual count-based method of myocardial wall brightening from diastole to systole. Nevertheless, the correlation of regional wall motion was good in mismatch patients, as well as in match patients (Table 4). The assessment of regional LV function, therefore, will be satisfactory when regional wall motion and thickening are considered together on BMIPP-gated SPECT.

Recently, we have reported the feasibility of BMIPP FPRNA acquired with a multicrystal gamma camera for the assessment of LV function (28). The correlation in LVEF between BMIPP-gated SPECT and FPRNA in this study ( $r = 0.95$ ) was comparable with that between BMIPP FPRNA and <sup>99m</sup>Tc-FPRNA in the previous study ( $r = 0.96$ ). However, BMIPP-gated SPECT is advantageous over BMIPP FPRNA, in that gated SPECT can be performed with a single-crystal camera widely available. Moreover, the technique of gated SPECT is three-dimensional, which will allow more precise regional assessment than FPRNA.

**Relationship Between Regional BMIPP Uptake and Left Ventricular Function**

It is well known that in patients with CAD wall motion abnormality is often associated with decreased BMIPP uptake in overall segmental analysis (4-7). However, it has

**TABLE 4**

Relationship in Regional Functional Scores Between BMIPP- and MIBI-Gated SPECT in Mismatch Patients

BMIPP functional scores	MIBI functional scores				Total
	0	1	2	3	
0	91/115	3/7	2/0	0/0	96/122
1	11/14	37/21	3/1	0/0	51/36
2	1/4	7/7	15/6	1/1	24/18
3	0/3	1/1	6/6	11/3	18/13
Total	103/136	48/36	26/13	12/4	189/189

BMIPP =  $\beta$ -methyl-p-iodophenyl-pentadecanoic acid; MIBI = methoxyisobutyl isonitrile.

Numbers of segments were expressed as wall motion score/wall-thickening score. Wall motion scores,  $\kappa = 0.707$ ,  $r = 0.853$ ,  $P < 0.0001$ ; wall-thickening scores,  $\kappa = 0.526$ ,  $r = 0.754$ ,  $P < 0.0001$ .

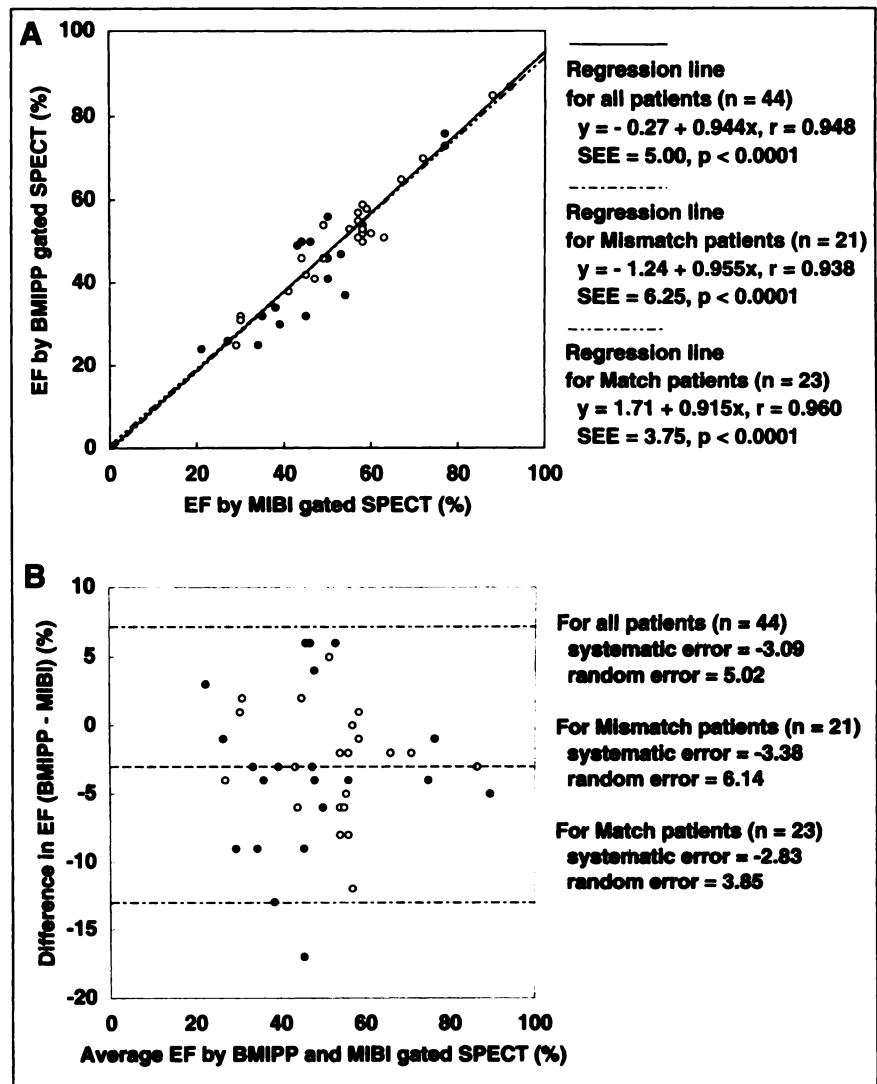


**FIGURE 3.** (A) Scatterplots for left ventricular ejection fraction (EF) obtained from  $^{123}\text{I}$ -BMIPP- and  $^{99\text{m}}\text{Tc}$ -methoxyisobutyl isonitrile (MIBI)-gated SPECT. (B) Bland-Altman plots for left ventricular EF obtained from BMIPP- and MIBI-gated SPECT. ● = mismatch patients; ○ = match patients.

also been reported that two kinds of inconsistent findings are sometimes observed: segments with good regional wall motion show severely reduced BMIPP uptake, and segments with severe regional dysfunction show preserved BMIPP uptake (4,8,9). Tamaki et al. (4) examined 28 patients with myocardial infarction and reported that 4 (2.0%) of 196 segments showed normal wall motion in spite of absent BMIPP uptake, and that 1 segment (0.5%) showed akinesis or dyskinesis in spite of normal BMIPP uptake. Knapp et al. (8) also reported that 2 (1.1%) each of 180 segments showed these controversial phenomena in 20 patients with CAD. Some of the reasons for the former phenomenon may be metabolic alteration (10) to maintain contraction and the recovery phase after prolonged ischemia (9), whereas the latter phenomenon may be related to enhanced BMIPP uptake higher than perfusion, possibly due to passive systolic wall stretch (11). Our data also support the finding that the severity of regional LV dysfunction is not necessarily identical with the degree of reduced BMIPP uptake in each segment in spite of significant overall correlation (Table 6). In addition, BMIPP uptake depends on various

factors, including regional myocardial blood flow, endogenous lipid pool (32), triglyceride synthesis (33) and adenosine triphosphate concentration (34). Our findings suggest that information on LV function obtained from BMIPP-gated SPECT is substantially different from that on fatty acid utilization, and combined assessment of them may be meaningful.

#### BMIPP SPECT Without Combined Use of a Perfusion Tracer

A fatty acid metabolic tracer of BMIPP provides different information from perfusion tracers. Previous studies have shown that mismatch between myocardial flow tracers and BMIPP uptake reflected myocardial viability in patients with myocardial infarction (4-13), in which cases resting perfusion images are always required.

There may be no need for applying gated technique to BMIPP SPECT to assess LV function if MIBI-gated SPECT is conducted for the same patient, because BMIPP-gated SPECT has little technical advantage over MIBI-gated SPECT. However, BMIPP SPECT can be useful in some

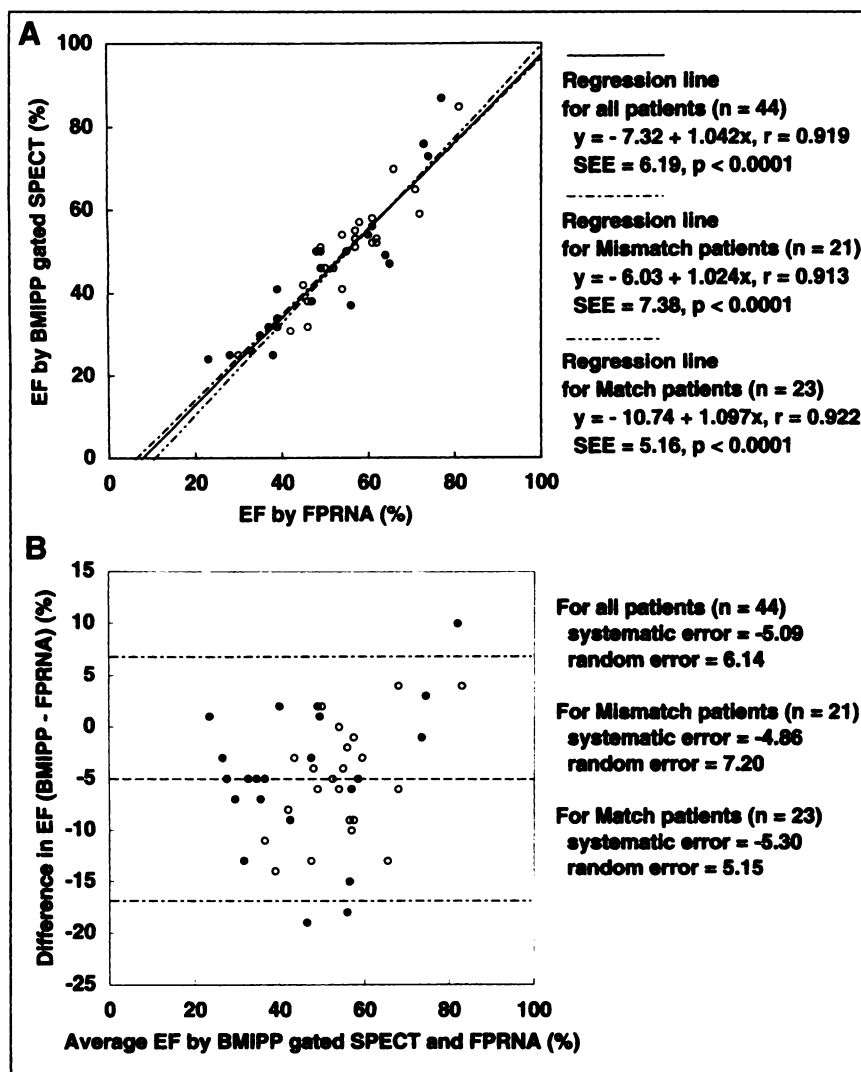


**FIGURE 4.** (A) Scatterplots for left ventricular ejection fraction (EF) obtained from  $^{123}\text{I}$ -BMIPP-gated SPECT and first-pass radionuclide angiography (FPRNA). (B) Bland-Altman plots for left ventricular EF obtained from BMIPP-gated SPECT and FPRNA. ● = mismatch patients; ○ = match patients.

clinical situations. First, a report indicated that initial distribution (2–5 min) of BMIPP accurately reflected myocardial perfusion in patients with acute coronary syndromes and that myocardial perfusion and fatty acid metabolism

could be evaluated simultaneously with only a single injection of BMIPP without using a perfusion tracer (14). Second, another report suggested that BMIPP washout rate was useful for identifying postangioplastic restenosis with-

**TABLE 6**

Relationship in Regional Defect Scores and Regional Functional Scores on BMIPP-Gated SPECT

BMIPP defect score	BMIPP functional scores				
	0	1	2	3	Total
0	193/234	45/35	16/1	16/0	270/270
1	45/56	27/16	10/18	8/0	90/90
2	1/6	7/6	10/4	4/6	22/22
3	5/0	3/0	4/2	2/12	14/14
Total	244/296	82/57	40/25	30/18	396/396

BMIPP =  $\beta$ -methyl-p-iodophenyl-pentadecanoic acid.

Numbers of segments were expressed as wall motion score/wall-thickening score. Wall motion scores,  $\kappa = 0.211$ ,  $r = 0.325$ ,  $P < 0.0001$ ; wall-thickening scores,  $\kappa = 0.275$ ,  $r = 0.495$ ,  $P < 0.0001$ .

**TABLE 7**

Relationship in Regional Defect Scores and Regional Functional Scores on MIBI-Gated SPECT

MIBI defect score	MIBI functional scores				
	0	1	2	3	Total
0	217/259	44/34	22/3	13/0	296/296
1	38/51	21/15	10/9	7/1	76/76
2	4/6	7/2	5/6	0/2	16/16
3	2/0	2/1	4/1	0/6	8/8
Total	261/316	74/52	41/19	20/9	396/396

MIBI = methoxyisobutyl isonitrile.

Numbers of segments were expressed as wall motion score/wall-thickening score. Wall motion scores,  $\kappa = 0.171$ ,  $r = 0.274$ ,  $P < 0.0001$ ; wall-thickening scores,  $\kappa = 0.261$ ,  $r = 0.390$ ,  $P < 0.0001$ .

out perfusion SPECT (15). Third, it is also reported that BMIPP SPECT is more sensitive for the detection of ischemic myocardium than perfusion SPECT (16–18), suggesting that perfusion studies may be omitted for the screening when BMIPP SPECT is normal. Fourth, in patients with cardiomyopathy, BMIPP uptake is known to be related to severity, prognosis and therapeutic effect (19–21), indicating that BMIPP SPECT should be the first consideration for following up these patients once CAD is excluded. Therefore, we believe that information on LV function obtained from BMIPP-gated SPECT can be effective in these situations without a perfusion tracer.

### Clinical Significance of BMIPP-Gated SPECT

One clinical value of gated SPECT is that regional tracer uptake and regional wall motion are assessed on the same sequence, which aids in distinguishing artifacts caused by attenuation (35–38) or by abnormal segmental contraction (39,40) from truly decreased tracer uptake. Strictly speaking, without applying gated technique to BMIPP SPECT, regional BMIPP uptake and wall motion cannot be estimated on the same slices, even when gated perfusion SPECT is performed separately. Therefore, BMIPP-gated SPECT may contribute to the accurate interpretation of BMIPP images.

Additionally, it is reported that myocardial fatty acid utilization is concerned with severity, prognosis and therapeutic effect (19–21), and LV function is also known as an important indicator of prognosis in patients with various cardiac diseases. The current study shows that BMIPP-gated SPECT has the potential to assess the two substantially different parameters simultaneously. BMIPP-gated SPECT may be useful for prognostic estimation, follow-up management or therapy planning by providing more comprehensive information, although further investigations with larger or more strictly selected patient populations may be required for determining its prognostic value.

Furthermore, the combined method of early (2–5 min) dynamic acquisition (14) and late gated acquisition of BMIPP SPECT has the potential to assess myocardial perfusion, free fatty acid utilization, and LV function simultaneously with a single injection of BMIPP without using perfusion tracers. This approach will be highly advantageous in patients with acute coronary disease when information is needed in a short period of time, and it will be especially advantageous in younger subjects whose radiation dose should be minimized. This approach will simplify cardiovascular radionuclide studies, which will lead to reduced costs and radiation doses for these patients.

### Potential Limitations

Because the injected dose of BMIPP (111 MBq) was approximately one fifth that of MIBI (600 MBq), we set the acquisition time at 60 s per projection for BMIPP-gated SPECT, compared to 40 s per projection for MIBI-gated SPECT. The total acquisition time of BMIPP-gated SPECT was about 16 min, which is considered acceptable for routine clinical studies. The total BMIPP myocardial counts

were approximately one half those of MIBI. In addition, areas of reduced BMIPP uptake compared with perfusion tracers (mismatch) were frequently observed in patients with CAD (Table 2). Accordingly, BMIPP-gated SPECT was thought to be disadvantageous for the assessment of LV function. Nevertheless, we found that the image quality and accuracy for evaluating functional parameters of BMIPP-gated SPECT were clinically acceptable.

We applied Germano's software in the same conditions for calculating LVEF for MIBI- and BMIPP-gated SPECT, despite the difference in radionuclide, because this technique is fully automatic and operators are not allowed to interfere with any operation of the algorithm to determine the endocardial surface even in low-uptake areas. Also, when Germano et al. (24) reported that their algorithm could be successfully applied to  $^{201}\text{Tl}$ -gated SPECT, there was no indication that they had to change the condition for  $^{201}\text{Tl}$ . Our data support strong agreement in functional parameters between MIBI- and BMIPP-gated SPECT.

### CONCLUSION

BMIPP-gated SPECT can accurately evaluate the regional and global LV function with the QGS software. BMIPP-gated SPECT offers the opportunity for the simultaneous assessment of myocardial fatty acid utilization, LV function and possibly myocardial perfusion. We believe that BMIPP-gated SPECT is valuable in respect to both diagnosis and prognosis and will simplify cardiovascular radionuclide studies leading to reduced costs and radiation doses in limited clinical situations.

### ACKNOWLEDGMENTS

We thank Emiko Komori, RT, Hiroshi Yokoyama, RT, Keiichi Matsumoto, RT, and Tohru Fujita, RT, at Kyoto University Hospital for technical assistance. We also thank Nisho Iwai Co., Ltd., and Philips Medical Systems Corporation for providing the SIM-400 system and the VariCam system, respectively.

### REFERENCES

1. Grucker D, Florentz P, Ozwald T, Chambron J. Myocardial gated tomoscintigraphy with  $^{99\text{m}}\text{Tc}$ -methoxy-isobutyl-isonitrile (MIBI): regional and temporal activity curve analysis. *Nucl Med Commun.* 1989;10:723–732.
2. Manning F, Morgan-Manning M. Gated SPECT with technetium-99m-sestamibi for assessment of myocardial perfusion abnormalities. *J Nucl Med.* 1993;34:601–608.
3. DePuey EG, Nichols K, Dobrinsky C. Left ventricular ejection fraction assessed from gated technetium-99m-sestamibi SPECT. *J Nucl Med.* 1993;34:1871–1876.
4. Tamaki N, Kawamoto M, Yonekura Y, et al. Regional metabolic abnormality in relation to perfusion and wall motion in patients with myocardial infarction: assessment with emission tomography using an iodinated branched fatty acid analog. *J Nucl Med.* 1992;33:659–667.
5. Franken PR, De Geeter F, Dendale P, Demoor D, Block P, Bossuyt A. Abnormal free fatty acid uptake in subacute myocardial infarction after coronary thrombolysis: correlation with wall motion and inotropic reserve. *J Nucl Med.* 1994;35:1758–1765.
6. Ito T, Tanouchi J, Kato J, et al. Recovery of impaired left ventricular function in patients with acute myocardial infarction is predicted by the discordance in defect size on  $^{123}\text{I}$ -BMIPP and  $^{201}\text{Tl}$  SPECT images. *Eur J Nucl Med.* 1996;23:917–923.

7. Taki J, Nakajima K, Matsunari I, et al. Assessment of improvement of myocardial fatty acid uptake and function after revascularization using iodine-123-BMIPP. *J Nucl Med.* 1997;38:1503–1510.
8. Knapp FF, Franken PR, Kropp J. Cardiac SPECT with iodine-123-labeled fatty acids: evaluation of myocardial viability with BMIPP. *J Nucl Med.* 1995;36:1022–1030.
9. Tateno M, Tamaki N, Magata Y, et al. Assessment of fatty acid uptake in ischemic heart disease without myocardial infarction. *J Nucl Med.* 1996;37:1981–1985.
10. Tamaki N, Tadamura E, Kawamoto M, et al. Decreased uptake of iodinated branched fatty acid analog indicates metabolic alternation in ischemic myocardium. *J Nucl Med.* 1995;36:1974–1980.
11. De Geeter F, Franken PR, Knapp FF, Bossuyt A. Relationship between blood flow and fatty acid metabolism in subacute myocardial infarction: a study by means of <sup>99m</sup>Tc-sestamibi and <sup>123</sup>I-beta-methyl-iodo-phenyl pentadecanoic acid. *Eur J Nucl Med.* 1994;21:283–291.
12. Kawamoto M, Tamaki N, Yonekura Y, et al. Combined study with I-123 fatty acid and thallium-201 to assess ischemic myocardium: comparison with thallium redistribution and glucose metabolism. *Ann Nucl Med.* 1994;8:47–54.
13. Tamaki N, Tadamura E, Kudoh T, et al. Prognostic value of iodine-123 labelled BMIPP fatty acid analogue imaging in patients with myocardial infarction. *Eur J Nucl Med.* 1996;23:272–279.
14. Kobayashi H, Kusakabe K, Momose M, et al. Evaluation of myocardial perfusion and fatty acid uptake using a single injection of iodine-123 BMIPP in patients with acute coronary syndrome. *J Nucl Med.* 1998;39:1117–1122.
15. Yoshida S, Ito M, Mitsunami K, Kinoshita M. Improved myocardial fatty acid metabolism after coronary angioplasty in chronic coronary artery disease. *J Nucl Med.* 1998;39:933–938.
16. Nakajima K, Shuke N, Nitta Y, et al. Comparison of <sup>99m</sup>Tc-pyrophosphate, <sup>201</sup>Tl perfusion, <sup>123</sup>I-labelled methyl-branched fatty acid and sympathetic imaging in acute coronary syndrome. *Nucl Med Commun.* 1995;16:494–503.
17. Nakajima K, Shimizu K, Taki J, et al. Utility of iodine-123-BMIPP in the diagnosis and follow-up of vasospastic angina. *J Nucl Med.* 1995;36:1934–1940.
18. Takeishi Y, Atsumi H, Fujiwara S, Takahashi K, Tomoike H. Fatty acid metabolic imaging with <sup>123</sup>I-BMIPP for the diagnosis of coronary artery disease: application to patients with diabetes mellitus and hyperlipidaemia. *Nucl Med Commun.* 1996;17:675–680.
19. Nishimura T, Nagata S, Uehara T, et al. Prognosis of hypertrophic cardiomyopathy: assessment by <sup>123</sup>I-BMIPP (beta-methyl-p-(<sup>123</sup>I)iodophenyl pentadecanoic acid) myocardial single photon emission computed tomography. *Ann Nucl Med.* 1996;10:71–78.
20. Kim Y, Sawada Y, Fujiwara G, Chiba H, Nishimura T. Therapeutic effect of co-enzyme Q10 on idiopathic dilated cardiomyopathy: assessment by iodine-123 labelled 15-(p-iodophenyl)-3(R,S)-methylpentadecanoic acid myocardial single-photon emission tomography. *Eur J Nucl Med.* 1997;24:629–634.
21. Tadamura E, Kudoh T, Hattori N, et al. Impairment of BMIPP uptake precedes abnormalities in oxygen and glucose metabolism in hypertrophic cardiomyopathy. *J Nucl Med.* 1998;39:390–396.
22. Germano G, Kiat H, Kavanagh P, et al. Automatic quantification of ejection fraction from gated myocardial perfusion SPECT. *J Nucl Med.* 1995;36:2138–2147.
23. Mazzanti M, Germano G, Kiat H, Friedman J, Berman D. Fast technetium-99m-labeled-sestamibi gated single-photon emission computed tomography for evaluation of myocardial function. *J Nucl Cardiol.* 1996;3:143–149.
24. Germano G, Erel J, Kiat H, Kavanagh P, Berman D. Quantitative LVEF and qualitative regional function from gated thallium-201 perfusion SPECT. *J Nucl Med.* 1997;38:749–754.
25. DePuey EG, Berger HJ. Evaluation of cardiac function using first pass radionuclide angiocardiology. In: Adam WE, ed. *Handbook of Nuclear Medicine.* Vol. 2. New York, NY: Gustav Fisher Verlag; 1993:103–126.
26. Esquerré JP, Coca FJ, Gantet P, Ouhayoun E. Feasibility of first-pass radionuclide angiography with a 10-mCi technetium bolus using a single-crystal digital gamma camera: implications for technetium-sestamibi single-day protocols. *Eur J Nucl Med.* 1995;22:521–527.
27. Takahashi N, Tamaki N, Tadamura E, et al. Combined assessment of regional perfusion and wall motion in patients with coronary artery disease with technetium 99m tetrofosmin. *J Nucl Cardiol.* 1994;1:29–38.
28. Tadamura E, Kitano H, Kudoh T, et al. First-pass radionuclide angiography using iodine-123 myocardial tracers and a multicrystal gamma camera. *J Nucl Med.* 1998;39:938–944.
29. Cohen J. A coefficient of agreement for normal scales. *Educ Psychol Meas.* 1960;20:37–46.
30. Bland J, Altman D. Statistical methods for assessing agreement between two methods of clinical measurement. *Lancet.* 1986;1:307–310.
31. Bland J, Altman D. A note on the use of the intraclass correlation coefficient on the evaluation of agreement between two methods of measurement. *Comput Biol Med.* 1990;20:337–340.
32. Knapp FF, Ambrose KR, Goodman MM. New radioiodinated methylbranched fatty acids for cardiac studies. *Eur J Nucl Med.* 1986;12:S39–S44.
33. Fujibayashi Y, Yonekura Y, Kawai K, et al. Basic studies on I-123-beta-methyl-p-iodophenylpentadecanoic acid (BMIPP) for myocardial functional diagnosis: effect of beta-oxidation inhibitor. *Jpn J Nucl Med.* 1988;25:1131–1135.
34. Fujibayashi Y, Yonekura Y, Takemura Y, et al. Myocardial accumulation of iodinated beta-methyl-branched fatty acid analogue, iodine-125-15-(p-iodophenyl)-3-(R,S)methylpentadecanoic acid (BMIPP), in relation to ATP concentration. *J Nucl Med.* 1990;31:1818–1822.
35. DePuey EG. How to detect and avoid myocardial perfusion SPECT artifacts. *J Nucl Med.* 1994;35:699–702.
36. Taillefer R, DePuey EG, Udelson JE, et al. Comparative diagnostic accuracy of Tl-201 and Tc-99m sestamibi SPECT imaging (perfusion and ECG-gated SPECT) in detecting coronary artery disease in women. *J Am Coll Cardiol.* 1997;29:69–77.
37. Smanio PE, Watson DD, Segalla DL, et al. Value of gating of technetium-99m sestamibi single-photon emission computed tomographic imaging. *J Am Coll Cardiol.* 1997;30:1687–1692.
38. Choi JY, Lee KH, Kim SJ, et al. Gating provides improved accuracy for differentiating artifacts from true lesions in equivocal fixed defects on technetium 99m tetrofosmin perfusion SPECT. *J Nucl Cardiol.* 1998;5:395–401.
39. Eisner RL, Schmarkey LS, Martin SE, et al. Defects on SPECT perfusion images can occur due to abnormal segmental contraction. *J Nucl Med.* 1994;35:638–643.
40. Sugihara H, Tamaki N, Nozawa M, et al. Septal perfusion and wall thickening in patients with left bundle branch block assessed by technetium-99m-sestamibi gated tomography. *J Nucl Med.* 1997;38:545–547.